Bioorganic & Medicinal Chemistry Letters 24 (2014) 360–366

Contents lists available at ScienceDirect

Bioorganic & Medicinal Chemistry Letters

journal homepage: www.elsevier.com/locate/bmcl

Identification through structure-based methods of a bacterial NAD$^+$-dependent DNA ligase inhibitor that avoids known resistance mutations

Kerry Murphy-Benenato [a,*], Hongming Wang [a], Helen M. McGuire [a], Hajnalka E. Davis [a], Ning Gao [b], D. Bryan Prince [b], Haris Jahic [b], Suzanne S. Stokes [a,†], P. Ann Boriack-Sjodin [b,‡]

[a] Department of Chemistry, Infection Innovative Medicines, AstraZeneca R&D Boston, 35 Gatehouse Dr., Waltham, MA 02451, United States
[b] Department of Bioscience, Infection Innovative Medicines, AstraZeneca R&D Boston, 35 Gatehouse Dr., Waltham, MA 02451, United States

ARTICLE INFO

Article history:
Received 13 September 2013
Accepted 4 November 2013
Available online 15 November 2013

Keywords:
NAD$^+$-dependent ligase
Adenosine
Thienopyridine
Resistance
Antibacterial

ABSTRACT

In an attempt to identify novel inhibitors of NAD$^+$-dependent DNA ligase (LigA) that are not affected by a known resistance mutation in the adenosine binding pocket, a detailed analysis of the binding sites of a variety of bacterial ligases was performed. This analysis revealed several similarities to the adenine binding region of kinases, which enabled a virtual screen of known kinase inhibitors. From this screen, a thienopyridine scaffold was identified that was shown to inhibit bacterial ligase. Further characterization through structure and enzymology revealed the compound was not affected by a previously disclosed resistance mutation in *Streptococcus pneumoniae* LigA, Leu75Phe. A subsequent medicinal chemistry program identified substitutions that resulted in an inhibitor with moderate activity across various Gram-positive bacterial LigA enzymes.

The availability of effective antibacterial agents for the treatment of serious Gram positive and Gram negative infections is declining due to the rise of resistance to these drugs.[1–3] Resistance to antibacterials can result from a number of mechanisms. Activation or upregulation of genes will affect the ability of the drug to enter or remain in the bacterial cell, and enzymatic modification of the inhibitor itself will affect its ability to interact with its target. Alternatively, resistance can result from mutations to the protein target of the inhibitor, which can prevent the inhibitor from binding while maintaining the enzyme's functionality required for cell growth. Development of new antibacterial agents which work by unique modes of action on known targets and/or by inhibiting novel targets is valuable due to the absence of pre-existing resistance to these agents in a clinical setting.

DNA ligase has long attracted interest as a novel antibacterial target.[4–14] It plays a key role in DNA replication, repair, and recombination, catalyzing phosphodiester bond formation at single- or double-stranded breaks in DNA. Unlike mammalian ligase, which utilizes ATP as a co-factor, the bacterial enzyme relies on NAD$^+$ to form the enzyme–AMP complex. This difference reduces the risk of cross-reactivity of the antibacterial agent, adding to the attractiveness of this target. NAD$^+$ dependent DNA ligase (LigA) activity is essential for bacterial survival in several pathogens, including *Staphylococcus aureus* (*S. aureus*), *Streptococcus pneumoniae* (*S. pneumoniae*), and *Escherichia coli* (*E. coli*).[4,15,16] In addition, inhibitors of LigA are efficacious in in vivo animal models of bacterial infection.[8,14] However, as with other single-gene bacterial targets, resistance to inhibitors of LigA has been observed.[17] Recent studies identified a mutation in *S. pneumoniae* LigA, Leu75Phe, which conferred resistance to a class of adenosine-based inhibitors.[18] The mutated residue is located in a hydrophobic tunnel near the active site of LigA (AMP binding region) occupied by the inhibitor but not utilized by the enzyme–AMP complex, allowing the enzyme to retain the activity needed for bacterial growth while avoiding inhibition by this inhibitor series. All known potent inhibitors of LigA to date occupy this hydrophobic tunnel and would therefore be affected.[8,9,11–14] Given this result, an inhibitor of LigA which binds in the envelope of the natural substrate would be expected to retain activity against Leu75Phe mutants and therefore have potential utility as a therapeutic antibacterial agent.

Examination of the binding mode of the adenosine ring of NAD$^+$ in LigA indicated similarities in substrate-protein interactions to small molecule inhibitors of kinases, another class of adenosine-binding enzymes that have been productive targets for drug discovery.[19–21] The similarities in the recognition elements of the binding sites, despite divergent three-dimensional structures,

* Corresponding author.
E-mail address: kerry.benenato@astrazeneca.com (K. Murphy-Benenato).
† Present address: Business Analytics, Strategic Development Networks, Vertex Pharmaceuticals, Inc., Cambridge, Massachusetts 02139, United States.
‡ Present address: Structural Biology, Molecular Discovery, Epizyme, Inc., Cambridge, Massachusetts 02139, United States.

0960-894X/$ - see front matter © 2013 Elsevier Ltd. All rights reserved.
http://dx.doi.org/10.1016/j.bmcl.2013.11.007

allowed alternative structure-based approaches to be utilized in the search for LigA inhibitors that would bypass known resistance mutations.[22–24]

Protein kinases, such as protein kinase A (PKA),[25] and LigA show no three-dimensional structural similarity in overall structure or in the substrate binding regions (Fig. 1). Several bacterial ligase structures were overlaid using the superposition tool in Maestro (Schrödinger, LLC, Portland, OR), which aligned the α-carbon atoms of the protein backbones, enabling the comparison of the ligase pockets and ultimately the selection of *Haemophilus influenzae* (*H. influenzae*) LigA as a representative structure for docking. The structures of the ligands in several ligase structures were aligned with the ligands in several kinase structures, to facilitate the comparison of the adenosine binding domains of ligase and kinase structures. An in-house X-ray crystal structure of *H. influenzae* LigA (data not shown) was prepared for docking using the protein preparation module of Maestro, which deleted crystallographic waters, and assigned protons (at pH 7.0) to the protein structure. The protonated receptor structure was energy minimized using the OPLS2001 force field, with convergence criteria of 0.3 Å RMSD. Glide software (Schrodinger, v45108, 2007) was used to generate docking grids in the binding site of the prepared ligase structure, using default parameters. The grid was constructed to fill a box of 18 × 18 × 18 Å^3, with an inner box size of 12 × 12 × 12 Å^3. Several hydrogen-bond acceptors and donors were defined during receptor grid generation, for use as constraints during the docking. These analyses revealed important similarities between these two diverse protein scaffolds and their interactions with adenosine, including a hydrogen bond donor/acceptor pair with the amine and N1 of the adenine base with protein residues, a hydrogen bond with the N7 nitrogen, and a ribose pocket engaged in hydrogen bonds with the sugar hydroxyl group(s) (Fig. 1).[26]

Kinases have been fruitful and successful targets for inhibitor design, and fragment libraries are well established as starting points for lead generation efforts.[27] A library of fragments known to bind to kinase hinge regions was selected for docking experiments in order to positively bias the potential to discover active compounds in a virtual screen against LigA. A virtual kinase scaffold library comprised of 53 fragments was obtained from the in-house chemical collection and from the literature. The fragments were protonated, and all likely ionization states (from pH 5 to 9) were enumerated using the LigPrep module in Maestro (Schrödinger, 2007). Finally, low energy conformations of the fragments were generated using LigPrep, ensuring that the specified chiralities of any stereocenters in the fragments were preserved.

The Glide program (Schrödinger, 2007) was used to perform flexible ligand docking of the fragment library against the structure of *H. influenzae* LigA. The default GlideSP parameters were used for the docking, with the additional constraints that each pose satisfy at least two of the hydrogen bonds defined during receptor grid generation and all poses satisfy the canonical kinase-inhibitor hydrogen-bonding interactions. Docking poses were ranked according to the number of hydrogen-bonding constraints that were satisfied. Additionally, to address resistance, hits were filtered to exclude those that either positioned atoms (i) outside of the substrate (AMP) envelope, or (ii) within the envelope of the Leu-Phe resistance mutation. To perform the filtering, a homology model of the Leu-Phe resistance mutation (18) was generated using the Prime program (Schrödinger, 2007). Multiple rotamers of the phenylalanine residue were sampled to identify a low energy conformation, after which the resulting structure was energy-minimized using default parameters and the OPLS2001 force field. The homology model was used to filter docking poses that might be especially sensitive to this mutation.

One of the hits from the virtual screen was thienopyridine **1** (Table 1).[28] This compound was predicted to make the key hydrogen bond interactions described above and bind within the conserved portion of the binding pocket in the resistant mutant. The compound was synthesized in two steps from known thienopyridine **3** (Scheme 1).[29] Addition of *para*-methoxybenzylamine

Table 1
Comparison of biochemical potency of thienopyridine **1** and adenosine **2** (18).

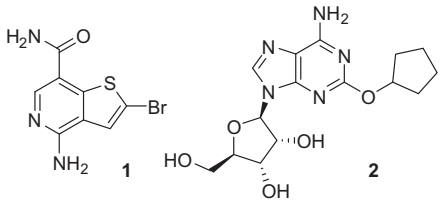

Compound	IC_{50} (μM)					MIC (μg/ml)
	Hin[a]	*Sau*[a]	*Efa*[a]	*Spn*[a]	*Spn* L75F[a]	*Spn*[a,c]
1	160	48	77	21	48	>64
2	0.51	0.43	NT[b]	0.21	33	8

[a] *Hin* = *H. influenzae*; *Sau* = *S. aureas*; *Efa* = *E. faecalis*; *Spn* = *S. pneumoniae* wild type; *Spn* L75F = *S. pneumoniae* L75F mutant.
[b] NT = not tested.
[c] ARC548.

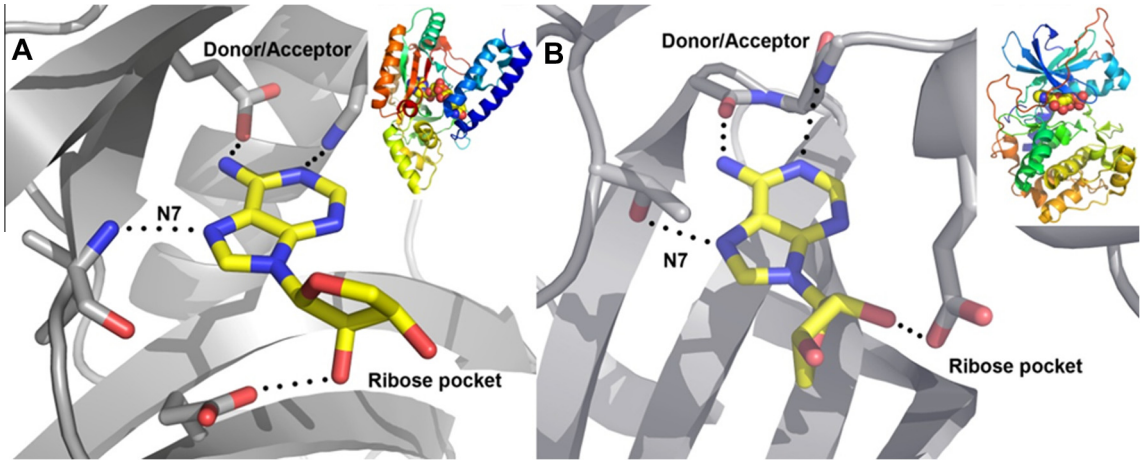

Figure 1. Comparison of LigA and PKA adenine binding sites. Hydrogen bond interactions between the adenine and ribose groups to (A) *E. faecalis* LigA (PDB code 1TAE) and (B) murine PKA (PDB code 1RDQ) (28) are shown as dotted lines and labeled. The overall three-dimensional structure of each protein is also shown in each panel.

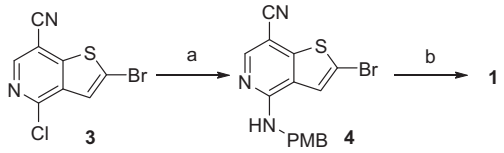

Scheme 1. Reagents and conditions: (a) $PMBNH_2$, K_2CO_3, NMP; (b) H_2SO_4.

to **3**, followed by hydrolysis with sulfuric acid afforded the desired product **1**. With thienopyridine **1** in hand, experiments were designed to address key questions: (1) does this kinase scaffold bind in the AMP-binding site of bacterial ligase, and if so (2) what would be the effect of the resistance mutation on binding affinity?

Thienopyridine **1** was tested for activity against a panel of LigA enzymes (Table 1). The compound was found to have IC_{50} values in the moderate to high μM range against *H. influenzae*, *S. aureus*, *Enterococcus faecalis (E. faecalis)*, and *S. pneumoniae*. Due to its moderate biochemical potency, compound **1** did not demonstrate any cellular activity against any bacterial species tested. These enzyme potencies are approximately 100-fold higher than an adenosine-based inhibitor **2** that incorporates a hydrophobic sidechain that occupies the hydrophobic pocket in which the resistant mutation Leu75Phe occurs[9] (Table 1); these compounds also show potency losses of >100-fold when tested biochemically against this resistance mutation. In contrast, when the thienopyridine compound **1** was tested for activity against the *S. pneumoniae* enzyme containing the Leu75Phe mutation, the inhibitor exhibited only a ~2-fold IC_{50} difference between the wild type and mutant proteins (Table 1). These results validate the methodologies used in the virtual screen, as the identified thienopyridine compound contained all the properties designed into the constraints used in the in silico screening including activity against both Gram positive and Gram negative isoforms of LigA (see Table 2).

A high resolution crystal structure of thienopyridine **1** bound to the adenylation domain of *E. faecalis* LigA is shown in Figure 2. Thienopyridine **1** bound in the adenosine binding site of the ligase protein, making the multiple hydrogen bonds (Fig. 2A) predicted by modeling. The amide makes a donor/acceptor interaction with Glu118 and Lys291, the thienopyridine nitrogen engages with the backbone NH of Ile121 and the amine interacts with the backbone carbonyl of Ile121. In addition to these hydrogen bonds, there is a π-stacking interaction between the thienopyridine ring and Tyr227. When overlaid with the *E. faecalis* LigA structure bound to NAD^+ (Fig. 2B),[30] it is clear that the thienopyridine scaffold occupies the same space in the binding pocket as the adenine base, and avoids the hydrophobic pocket where the Leu75Phe resistance mutation occurs in *S. pneumoniae* (equivalent to Leu89 in *E. faecalis*). The crystal structure of thienopyridine **1** was also solved in the *H. influenzae* isozyme and was found to bind identically in both proteins (data not shown). This result was not unexpected due to the previous observations regarding the similarities of the LigA binding site and allowed the higher resolution *E. faecalis* crystal system to be used for SAR development.

The thienopyridine scaffold was an attractive starting point for optimization.[31] The lead compound had low molecular weight (MW = 272), good physical properties (calculated log*P* = 1.57) excellent ligand efficiency (LE = 0.455),[32] and the core offered multiple points for diversification (Fig. 3). Guided by the experimentally determined structure and modeling, two main areas of the molecule were targeted for improvement of the biochemical potency: (1) building a new interaction with the Tyr87 loop via R^1 (Figs. 2 and 3), and (2) creating new interactions in the ribose pocket through R^2 and R^3 substitutions.

The chemistry to access these compounds is highlighted in Schemes 2–5. Analogs with R^1 variation (Fig. 3) could be accessed

Table 2
Crystallographic data collection and refinement statistics

Compound	**1**	**5c**
PDB code[a]	4LH6	4LH7
Space group	C222(1)	C222(1)
Cell constants a, b, c (Å) A, B, γ (°)	49.0, 104.4, 136.7 90.0, 90.0, 90.0	48.8, 105.0, 136.1 90.0, 90.0, 90.0
Resolution range (Å)	52.19–1.65	48.99–1.90
(Highest resolution shell)	(1.71–1.65)	(1.97–1.90)
Completeness overall (%)	98.9 (94.0)	95.8 (91.7)
Reflections, unique	42.077	26.859
Multiplicity	4.6 (3.3)	4.4 (4.5)
I/σ	11.9 (2.2)	9.9 (4.0)
$R_{\text{merge overall}}$[b]	0.058 (0.436)	0.102 (0.249)
$R_{\text{value overall}}$ (%)[c]	22.4	22.5
$R_{\text{value free}}$ (%)	25.4	25.9
Non hydrogen protein atoms	2659	2621
Non hydrogen ligand atoms (INH)	14	16
Non hydrogen ligand atoms (NMN)	22	22
Solvent molecules	253	159
R.m.s. deviations from ideal values		
Bond lengths (Å)	0.006	0.006
Bond angles (°)	0.960	0.992
Average *B* values (Å^2)		
Protein main chain atoms	26.3	24.7
Protein all atoms	27.0	25.5
Ligand (Compound)	34.0	25.0
Ligand (NMN)	28.6	31.9
Solvent	36.3	34.2
Φ, Ψ angle distribution for residues[d]		
In most favoured regions (%)	95.1	96.1
In additional allowed regions (%)	4.9	3.9
In generously regions (%)	0.0	0.0
In disallowed regions (%)	0.0	0.0

R_{free} is the cross-validation R factor computed for the test set of 5% of unique reflections.
[a] Coordinates have been deposited in the Protein Data Bank.
[b] $R_{\text{merge}} = \sum_{hkl}[(\sum_i |I_i - \langle I \rangle|)/\sum_i I_i]$.
[c] $R_{\text{value}} = \sum_{hkl}||F_{obs}| - |F_{calc}||/\sum_{hkl}|F_{obs}|$.
[d] Ramachandran statistics as defined by PROCHECK.

starting from **1**, **3**, or **4** (see Scheme 2). The bromine atom allowed for a diversity of chemistry: Zn(0) insertion (**5a**), Pd-catalyzed Negishi reaction (**5b**), nitrile displacement with CuCN (**5c**), Pd-catalyzed carbonylation (**5d**, **5e**), and Pd-catalyzed Suzuki reaction (**5f**). Beginning with Br intermediate **13** (Scheme 3),[28] analogous chemistry allowed access to R^2 variation (see **16a**, **16c** and **16d**). En route to **16c**, nitrile hydrolysis was observed when *para*-methoxybenzylamine was introduced, presumably due to advantageous water present in the reaction. Methyl substituted thienopyridine **16b** was synthesized from chloropyridine **17**.[33] Utilizing intermediate **3**, a variety of amines were introduced, offering R^3 diversity (**23a** and **23b**, Scheme 4). Finally disubstituted thienopyridine **24** was synthesized by bromination of intermediate **19** (Scheme 5).

With access to a diversity of analogs, we examined their ability to inhibit a panel of Gram positive NAD^+-dependent DNA ligase enzymes. The data is summarized in Table 3. Similar to compound **1**, the compounds tended to be more active against the Gram positive isozymes and none of the compounds demonstrated comparable activity against *H. influenzae*. The active sites of the *H. influenzae* and *E. faecalis* LigA proteins are extremely similar in overall structure (Cα RMSD of adenosine binding region ~0.78 Å^2) and in amino acid composition. Yet differences in potencies were seen between the Gram positive enzymes and *H. influenzae* enzyme tested due to the subtle differences in the active site structures, highlighting the potential challenge of finding a potent inhibitor for both Gram positive and Gram negative LigA enzymes.

Compounds **5a**–**5f** were designed to understand the effect of the Br and to target new interactions with Tyr87. Removal of the

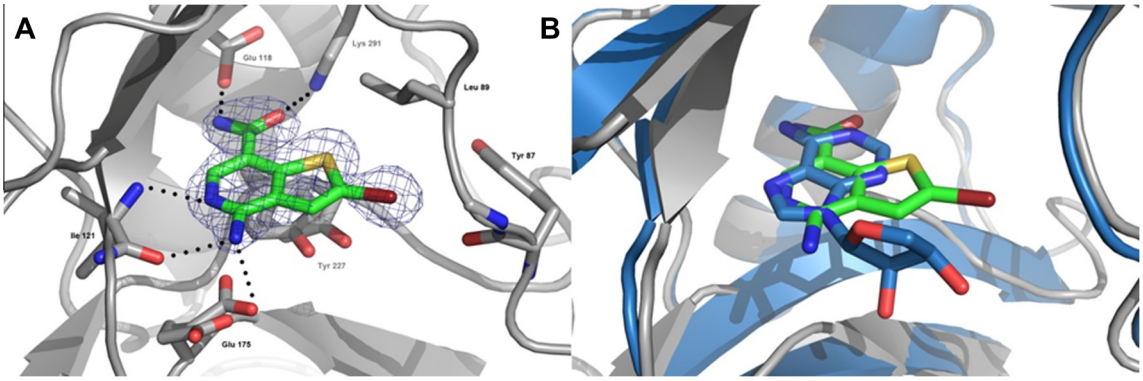

Fig. 2. Crystal structure of **1** bound to *E. faecalis* LigA. (A) Final 2Fo-Fc electron density (1.0σ) is shown superimposed on the final structure. Hydrogen bonds are shown as dotted lines. (B) Superposition of **1** (green/grey) with *E. faecalis* LigA bound to NAD^+ (blue, PDB code 1TAE) (37). For simplicity, only the adenine and ribose moieties of NAD^+ are shown in the figure.

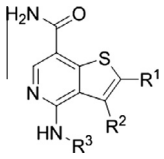

Fig. 3. Thienopyridine points of diversity.

Br (**5a**) or introduction of a small alkyl group (**5b**) reduced potency. Improvement was observed when electron-withdrawing functionalities with H-bond donors and acceptors were introduced (**5c**, **5d**). Amide **5c** afforded a twofold improvement in potency against the Gram positive enzymes as compared to bromide **1**, indicating a new interaction had potentially formed. This was confirmed by the crystal structure of compound **5c** in *E. faecalis* LigA, where a

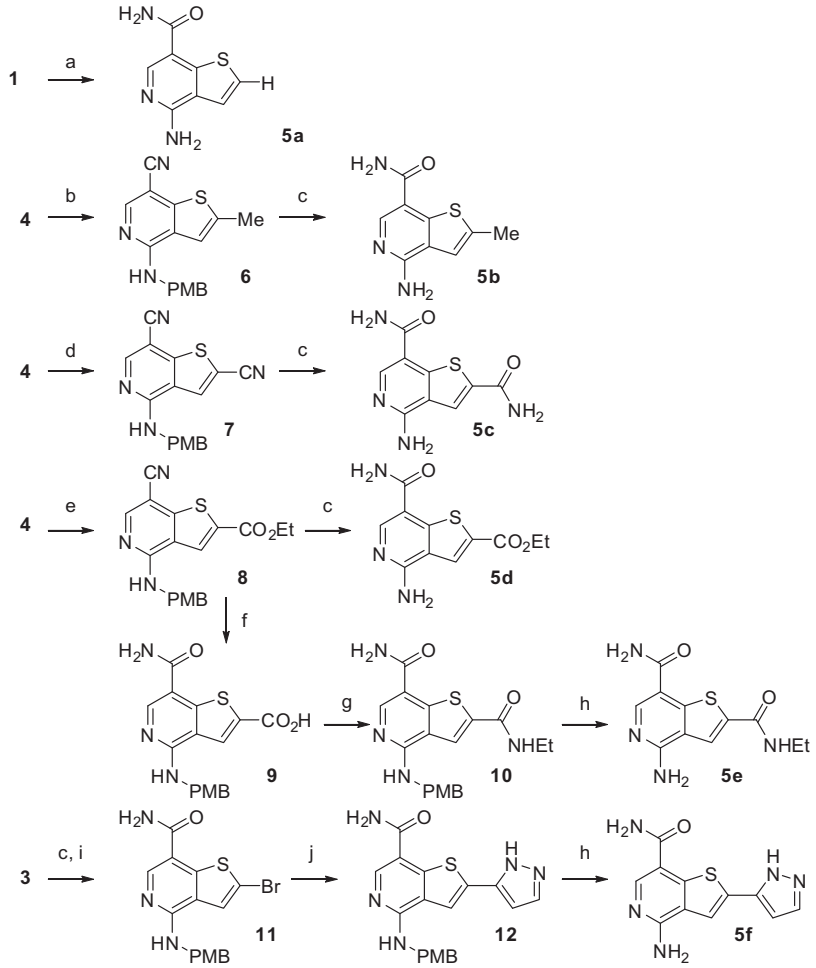

Scheme 2. Reagents and conditions: (a) Zn dust, AcOH, H_2O, *n*-propanol, 105 °C, 24 h; (b) MeZnBr, $Pd(PPh_3)_4$, THF, 65 °C, 18 h; (c) H_2SO_4, 2–3 h; (d) CuCN, DMF, 155 °C, 15 h; (e) CO, $Pd(PPh_3)_4$, Et_3N, EtOH, 75 °C, 40 h; (f) NaOH, THF/EtOH, 50 °C, 18 h; (g) $EtNH_2$, HATU, DIPEA, DMF, 48 h; (h) TFA, 50 °C, 18 h; (i) $PMBNH_2$, K_2CO_3, NMP, 120 °C, 1.5 h; (j) 1*H*-pyrazol-5-ylboronic acid, $Pd(PPh_3)_4$, $NaHCO_3$, dioxane/H_2O, 150 °C, 20 min.

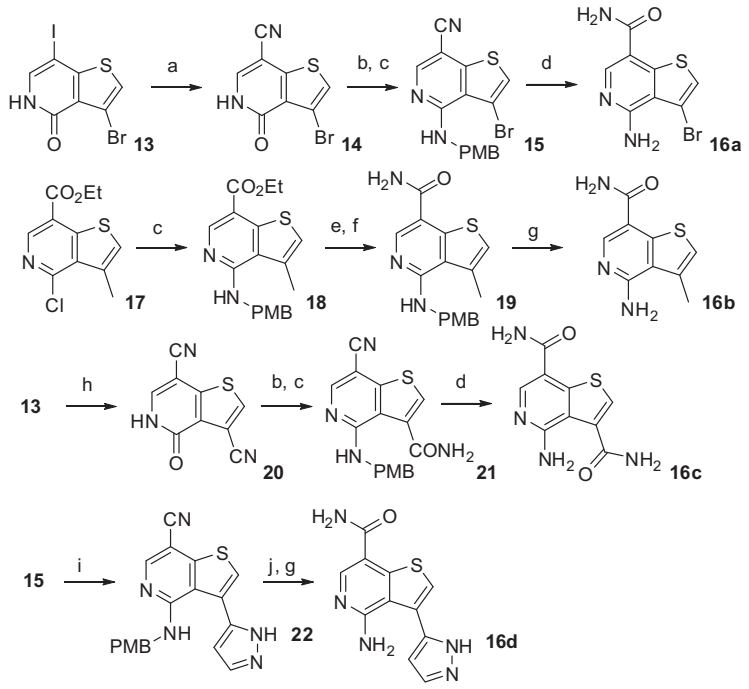

Scheme 3. Reagents and conditions: (a) $PdCl_2$, dppf, $Zn(CN)_2$, Zn dust, NMP, 110 °C, 14 h; (b) $POCl_3$, 110 °C, 18 h; (c) $PMBNH_2$, K_2CO_3, NMP, 110 °C, 3 h; (d) H_2SO_4, 1 h; (e) NaOH, THF/MeOH, 50 °C, 2 h; (f) NH_3, HATU, DIPEA, DMF, 2 h; (g) TFA, 50 °C, 1 h; (h) CuCN, DMF; (i) 1*H*-pyrazol-5-ylboronic acid, $Pd(PPh_3)_4$, Na_2CO_3, dioxane/water, 150 °C 30 min; (j) NaOH, EtOH/H_2O, 65 °C, 1 h.

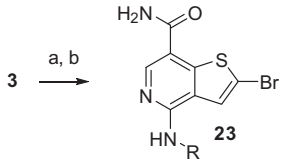

Scheme 4. Reagents and conditions: (a) H_2SO_4, 1 h; (b) RNH_2, 130 °C, 1 h.

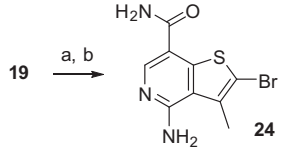

Scheme 5. Reagents and conditions: (a) NBS, $CHCl_3$, AcOH, 30 min; (b) TFA, 50 °C, 1 h.

new hydrogen bond between Tyr87 and the amide was observed (Fig. 4). Ester **5d** also demonstrated improved potency; however the structure of this compound bound to *E. faecalis* indicated no additional interactions and no confirmed density for the ester functionality (data not shown). In addition, when tested against the *S. pneumoniae* Leu75Phe mutant, a greater than 20-fold decrease in activity was observed (IC_{50} = >200 μM). It is postulated that the jump in IC_{50} for ester **5d** is due to the alkyl group being aimed outside of the natural substrate's binding pocket, toward the hydrophobic pocket, an area that had previously been exploited to achieve increased potency with LigA inhibitors.[9,11,12] This is supported by the loss of activity against the mutant enzyme. Attempts to introduce substituted amides (**5e**) resulted in diminished potency as compared to amide **5c**, perhaps due to loss of the H-bond and size constraints in that area of the pocket. In general aryl and heterocycle substitution, as exemplified by pyrazole **5f**, was comparable to Br (**2**), indicating the importance of π–π interactions.

Efforts to build into the ribose pocket of the enzyme through R^2 and R^3 variations met with little success. Compounds with R^2 diversity show the same trend as the analogous R^1 analogues, but with diminished potency (**16a**–**16d**, Table 3). Substituting heterocycles at R^2 (**16d**) gave a large decrease in activity as compared to R^1 (**5f**), possibly due to a shift of the compound within the pocket. R^3 analogues (**23a**–**23c**) showed no improvement in activity, which may be explained by disruption of the backbone hydrogen bond with Ile121.

The best result was observed when disubstitution on the thiophene ring was introduced (R^1 and $R^2 \neq$ H, **24**, Table 3). Compound **24** showed >fivefold increase in biochemical potency as compared with the mono–bromo compound **1** and >100-fold increase as compared to mono-methyl compound **16b**, however no improvement in *H. influenzae* potency. Potentially disubstitution is locking the ligand into the pocket as reflected by the ligand efficiency (LE = 0.50).[32,34] The activity of compound **24** was measured against the *S. pneumoniae* Leu75Phe resistance mutant with an IC_{50} value of 37 μM. The increase in the IC_{50} value when compared to the wild type enzyme is higher than the twofold increase seen for compound **1**, but significantly less shifted than the adenosine series. Though physical properties of compound **24** (>20-fold decrease in solubility, unpublished results) are not as optimal as the original hit **1**, the lead is still in the ideal molecular space (MW = 286, calculated log*P* = 2.07).[31]

The thienopyridine compounds did not achieve the levels of biochemical activity that would be expected to result in cellular activity against either Gram positive or Gram negative bacteria in vitro (observed MICs >200 μg/ml, data not shown). Due to the desire to avoid the synthesis of compounds with increased potential for resistance generation, the hydrophobic pocket within the binding site of LigA, previously shown to be effective in driving down biochemical potency[9] but outside the substrate molecular envelope, was avoided. With this vector eliminated from consideration we were unsuccessful in obtaining compounds of acceptable potency. Additionally, though we achieved an increase

Table 3
Biochemical potency of thienopyridine inhibitors of LigA

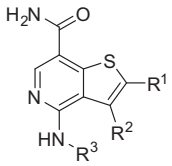

Compound	R^1	R^2	R^3	IC_{50} (μM)			
				Spn[a]	*Sau*[a]	*Efa*[a]	*Hin*[a]
1	Br	H	H	21	48	77	160
5a	H	H	H	25	>200	>200	>200
5b	Me	H	H	200	>200	>200	>200
5c	$CONH_2$	H	H	9.4	15	34	>200
5d	CO_2Et	H	H	9.4	8.9	74	>200
5e	CONHEt	H	H	140	75	>200	>200
5f	1*H*-Pyrazol-5-yl	H	H	29	36	100	>200
16a	H	Br	H	36	39	130	>200
16b	H	Me	H	>140	>200	>200	>200
16c	H	$CONH_2$	H	52	69	>200	>200
16d	H	1*H*-Pyrazol-5-yl	H	100	>200	>200	>200
23a	Br	H	*n*-Pr	150	180	130	200
23b	Br	H	Ph	>200	150	160	160
23c	Br	H	$(CH_2)_2OH$	>200	>200	>200	>200
24	Br	Me	H	3.1	7.1	8.1	>200

[a] *Sau* = *S. aureus*; *Efa* = *E. faecalis*; *Spn* = *S. pneumoniae* wild type; *Hin* = *H. influenzae*.

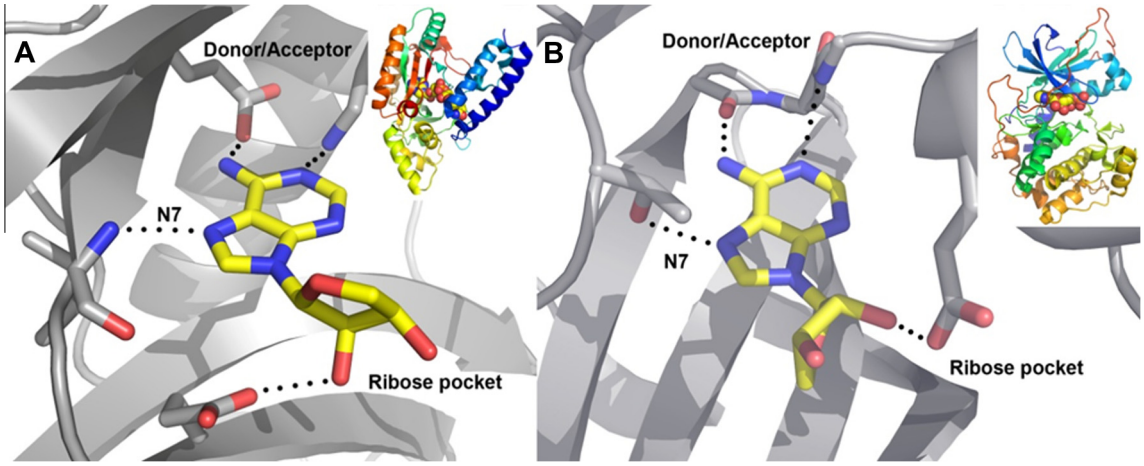

Fig. 4. Crystal structure of **5c** with *E. faecalis* LigA. Final 2Fo-Fc electron density (1.0σ) is shown superimposed on the final structure. Hydrogen bonds are shown as dotted lines.

in biochemical potency of the thienopyridine against wild type ligase, there was no improvement in IC_{50}'s against the *S. pneumoniae* Leu75Phe mutant (48 uM for compound **1** vs 37 uM for compound **24**). We were unable to obtain a crystal structure of the *S. pneumoniae* mutant enzyme, but we hypothesize there are other changes in the binding site of the mutant affecting binding.

Design of novel ligase inhibitors promises to be useful in antibacterial drug discovery. However attempts to develop potent inhibitors of the enzyme have been challenging. One recurrent problem in discovery efforts has been the development of drug resistance through mutations in the active site of the enzyme. These changes reduce the affinity of the inhibitor in the active site but permit the enzyme to function normally. In searching for novel inhibitors of this class of enzymes, we discovered a new scaffold based upon our previous knowledge of kinase inhibitors. The initial hypothesis that the adenosine binding sites of both ligase and kinases have some features in common allowed the use of scaffolds previously identified for kinase inhibition to probe the ligase binding site. Using virtual screening and modeling methods, a thienopyridine compound was identified that was not only active in ligase but also showed an improved biochemical profile against the LigA mutant found in resistant bacteria. This was supported by structural work done with *E. faecalis* ligase. The scaffold offered multiple opportunities for diversification and a robust structural system was developed that enabled iterative rounds of structure-based design and testing.

The starting point, compound **1**, demonstrated μM IC_{50}'s against Gram-positive DNA ligases and was shown through crystallographic and biochemical means to bind in the pocket of the natural substrate and not be affected by the Leu → Phe resistance mutation. Through chemical exploration and crystallography efforts, different substitutions were identified which improved the biochemical potency. A new hydrogen bond was introduced with the Tyr87 loop with the amide compound **5d**. In addition, opportunities were identified to improve the potency via disubstituted thiophenes (**24**). Unfortunately we were unable to optimize the

potencies to levels which would enable us to achieve cellular activity and validate the improved resistance profile of this series. Significant work still needs to be done in order to determine whether a LigA inhibitor with useful levels of potency that does not occupy the hydrophobic pocket can be developed.

The strategy employed to identify a new LigA inhibitor scaffold can be applied to other classes of enzymes that are not structurally related, requiring only observations of the topology of the enzyme binding site to generate useful hypotheses. For example, azaindole-based inhibitors of the bacterial topoisomerases were identified by using a kinase library by exploiting the donor/acceptor motif seen in ATP and other inhibitor classes.[24] The rapid discovery of alternative scaffolds using small virtual libraries could lead to significant cost and time savings when compared to high-throughput screening methodologies.

Acknowledgments

The authors thank Dr. Demetri Moustakas, Dr. Michael Hale and Dr. John Manchester for critical reading of the manuscript and Dr. Paul Lyne and Dr. Claudio Chuaqui for assembly of the kinase fragment library.

Supplementary data

Supplementary data (details on the purification of full length *E. faecalis* ligase, the purification of *E. faecalis* ligase adenylation domain, the deadenylation of *E. faecalis* ligase adenylation domain, crystallography and the synthesis of compounds **1**, **5a–f**, **16a–d**, **23a–c**, and **24**) associated with this article can be found, in the online version, at http://dx.doi.org/10.1016/j.bmcl.2013.11.007.

References and notes

1. Payne, D. J.; Gwynn, M. N.; Holmes, D. J.; Pompliano, D. L. *Nat. Rev. Drug Disc.* **2007**, *6*, 29.
2. Silver, L. L. *Clin. Microbiol. Rev.* **2011**, *24*, 71.
3. Alekshun, M. N.; Levy, S. B. *Cell* **2007**, *128*, 1037.
4. Lehman, I. R. *Science* **1974**, *186*, 790.
5. Brötz-Oesterhelt, H.; Knezevic, I.; Bartel, S.; Lampe, T.; Warnecke-Eberz, U.; Ziegelbauer, K.; Häbich, D.; Labischinski, H. *J. Biol. Chem.* **2003**, *278*, 39435.
6. Meier, T. I.; Yan, D.; Peery, R. B.; McAllister, K. A.; Zook, C.; Peng, S.-P.; Zhao, G. *FEBS J.* **2008**, *275*, 5258.
7. Ciarrocchi, G.; MacPhee, D. G.; Deady, L. W.; Tilley, L. *Antimicrob. Agents Chemother.* **1999**, *43*, 2766.
8. Mills, S. D.; Eakin, A. E.; Buurman, E. T.; Newman, J. V.; Gao, N.; Huynh, H.; Johnson, K. D.; Lahiri, S.; Shapiro, A. B.; Walkup, G. K.; Yang, W.; Stokes, S. S. *Antimicrob. Agents Chemother.* **2011**, *55*, 1088.
9. Stokes, S. S.; Huynh, H.; Gowravaram, M.; Albert, R.; Cavero-Tomas, M.; Chen, B.; Harang, J.; Loch, J. T.; Lu, M.; Mullen, G. B.; Zhao, S.; Liu, C.-F. *Bioorg. Med. Chem. Lett.* **2011**, *21*, 4556.
10. Tripathi, R. P.; Pandey, J.; Kukshal, V.; Ajay, A.; Mishra, M.; Dube, D.; Chopra, D.; Dwivedi, R.; Chaturvedi, V.; Ramachandran, R. *Med. Chem. Commun.* **2011**, *2*, 371.
11. Gu, W.; Wang, T.; Maltais, F.; Ledford, B.; Kennedy, J.; Wei, Y.; Gross, C. H.; Parsons, J.; Duncan, L.; Ryan, A. S. J.; Moody, C.; Perola, E.; Green, J. *Bioorg. Med. Chem. Lett.* **2012**, *22*, 3693.
12. Wang, T.; Duncan, L.; Gu, W.; O'Dowd, H.; Wei, Y.; Perola, E.; Parsons, J.; Gross, C. H.; Moody, C. S.; Ryan, A. S. J.; Charifson, P. S. *Bioorg. Med. Chem. Lett.* **2012**, *22*, 3699.
13. Buurman, E. T.; Laganas, V. A.; Liu, C. F.; Manchester, J. I. *ACS Med. Chem. Lett.* **2012**, *3*, 663.
14. Surivet, J.-P.; Lange, R.; Hubschwerlen, C.; Keck, W.; Specklin, J.-L.; Ritz, D.; Bur, D.; Locher, H.; Seiler, P.; Strasser, D. S.; Prade, L.; Kohl, C.; Schmitt, C.; Chapoux, G.; Ilhan, E.; Ekambaram, N.; Athanasiou, A.; Knezevic, A.; Sabato, D.; Chambovey, A.; Gaertner, M.; Enderlin, M.; Boehme, M.; Sippel, V.; Wyss, P. *Bioorg. Med. Chem. Lett.* **2012**, *22*, 6705.
15. Tomkinson, A. E.; Vijayakumar, S.; Pascal, J. M.; Ellenberger, T. *Chem. Rev.* **2012**, *106*, 687.
16. Shuman, S. *J. Biol. Chem.* **2009**, *284*, 17365.
17. Silver, L. *Nat. Rev. Drug Disc.* **2007**, *6*, 41.
18. Jahic, H.; Liu, C. F.; Thresher, J.; Livchak, S.; Wang, H.; Ehmann, D. *Biochem. Pharmacol.* **2012**, *84*, 654.
19. van Montfort, R. L.; Workman, P. *Trends Biotechnol.* **2009**, *27*, 315.
20. Grant, S. K. *Cell Mol. Life Sci.* **2009**, *66*, 1163.
21. Singh, J.; Petter, R. C.; Kluge, A. F. *Curr. Opin. Chem. Biol.* **2010**, *14*, 475.
22. Miller, J. R.; Dunham, S.; Mochalkin, I.; Banotai, C.; Bowman, M.; Buist, S.; Dunkle, B.; Hanna, D.; Harwood, J.; Huband, M. D.; Karnovsky, A.; Kuhn, M.; Limberakis, C.; Liu, J. Y.; Mehrens, S.; Mueller, W. T.; Narasimhan, L.; Ogden, A.; Ohren, J.; Vara, P. J. V. N.; Shelly, J. A.; Skerlos, L.; Sulavik, M.; Thomas, V. H.; VanderRoest, S.; Wang, L.; Wang, Z.; Whitton, A.; Zhu, T.; Stover, C. K. *Proc. Natl. Acad. Sci. U.S.A.* **2009**, *106*, 1737.
23. Mochalkin, I.; Miller, J. R.; Narasimhan, L.; Thanabal, V.; Erdman, P.; Cox, P. B.; Prasad, J. V. N. V.; Lightle, S.; Huband, M. D.; Stover, C. K. *ACS Chem. Biol.* **2009**, *4*, 473.
24. Manchester, J. I.; Dussault, D. D.; Rose, J. A.; Boriack-Sjodin, P. A.; Uria-Nickelsen, M.; Ioannidis, G.; Bist, S.; Fleming, P.; Hull, K. G. *Bioorg. Med. Chem. Lett.* **2012**, *22*, 5150.
25. Yang, J.; Ten, E.; Lynn, F.; Xuong, N.; Taylor, S. S. *J. Mol. Biol.* **2004**, *336*, 473.
26. Ghose, A. K.; Herbertz, T.; Pippin, D. A.; Salvino, J. M.; Mallamo, J. P. *J. Med. Chem.* **2008**, *5*, 5149.
27. de Kloe, G. E.; Bailey, D.; Leurs, R.; de Esch, I. J. *Drug Discovery Today* **2009**, *14*, 630.
28. Abbott, L.; Betschmann, P.; Burchat, A.; Calderwood, D. J.; Davis, H.; Hrnciar, P.; Hirst, G. C.; Li, B.; Morytko, M.; Mullen, K.; Yang, B. *Bioorg. Med. Chem. Lett.* **2007**, *17*, 1167.
29. Talamas F.X., Wang B. WO2005105809A1, 2005.
30. Gajiwala, K. S.; Pinko, C. *Structure* **2004**, *12*, 1449.
31. Rees, D. C.; Congreve, M.; Murray, C. W.; Carr, R. *Nat. Rev. Drug Disc.* **2004**, *3*, 660.
32. Schultes, S.; de Graaf, C.; Haasksma, E. E. J.; de Esch, I. J. P.; Leurs, R.; Krämer, O. *Drug Discovery Today* **2010**, *7*, 157.
33. Luk K., Mcdermott L.A., Rossman P.L., Wovkulich P.M., Zhang Z. US20050256154A1, 2005.
34. Orita, M.; Ohno, K.; Niimi, T. *Drug Discovery Today* **2009**, *14*, 321.